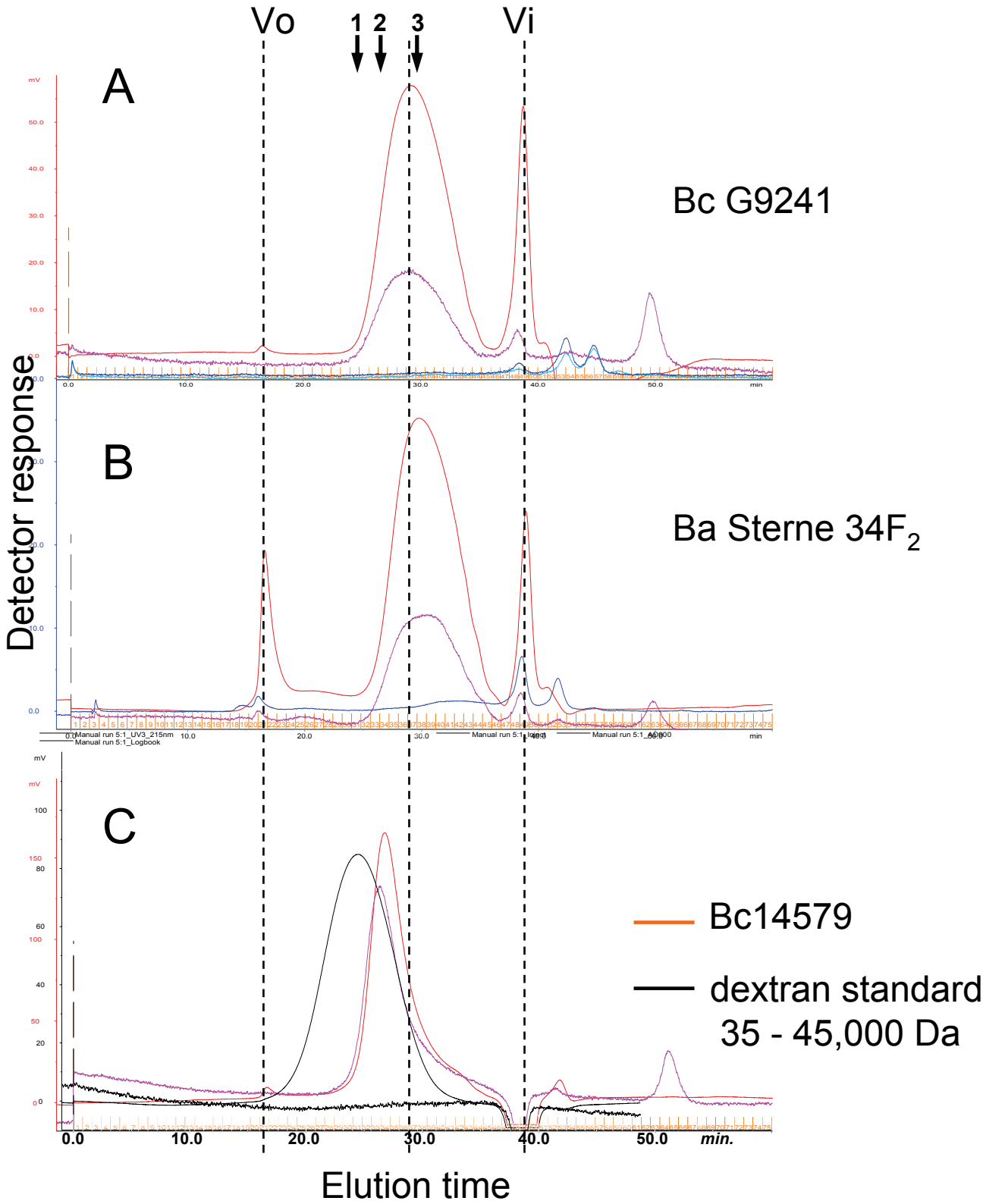

Supplemental Fig. S1

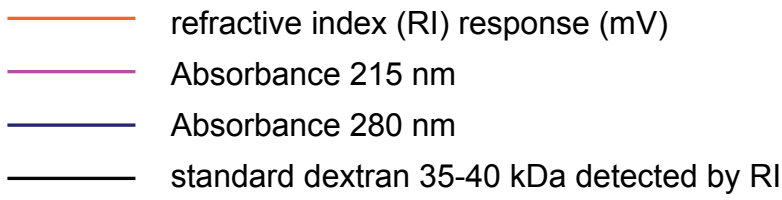

Supplemental Fig. S1

Purification and molecular mass estimation of the SCWP isolated from different *Bacillus* strains. SCWPs were released from cell walls by treatment with hydrofluoric acid, dialyzed, then chromatographed on a Superose-12 FPLC size exclusion column, in comparison to standard $\alpha 1 \rightarrow 6$ linked dextrans. ***A***, *B. cereus* G9241. ***B***, *B. anthracis* Sterne 34F2. ***C***, type strain *B. cereus* ATCC14579. The SCWP from the pathogenic *B. cereus* and *B. anthracis* strains elute at approximately the same location, between the 25 kDa and 11 kDa dextran standards, (K_{av} = 0.411, calc. mass 12,040 Da). The elution profile of *B. cereus* 03BB87 SCWP was essentially identical to that of *Bc*G9241, while *Bc* 03BB102 SCWP had K_{av} = 0.448, calc. mass 9,370 Da (not shown). For comparison, the non-pathogenic *B. cereus* type strain ATCC14579 SCWP elutes slightly after the 25 kDa dextran, (K_{av} = 0.337; calc. mass 20,020 Da). The *Bacillus* SCWP preparations, in particular those from *B. anthracis*, contain variable amounts of a high molecular weight glucan which elutes at the void volume (Vo). Glycosyl composition and NMR analysis (COSY, TOCSY, HSQC) indicated that in all strains it was exclusively a polysaccharide composed of glucose in predominately $\alpha 1 \rightarrow 4$ linkage. This glucan was most prevalent in the *B. anthracis* strains, and may correspond to a glycogen storage polysaccharide reported previously in certain *B. cereus* and other *Bacillus* strains. Column total inclusion volume, (Vi). In addition to the 35-45 kDa dextran profile, the elution positions of the 25 kDa and 11 kDa dextrans are indicated (**1**= 35-45 kDa; **2** = 25 kDa; **3** = 11 kDa). Molecular mass of SCWPs were estimated by comparing their observed K_{av} with those of standard dextrans, plotted vs. log MW.

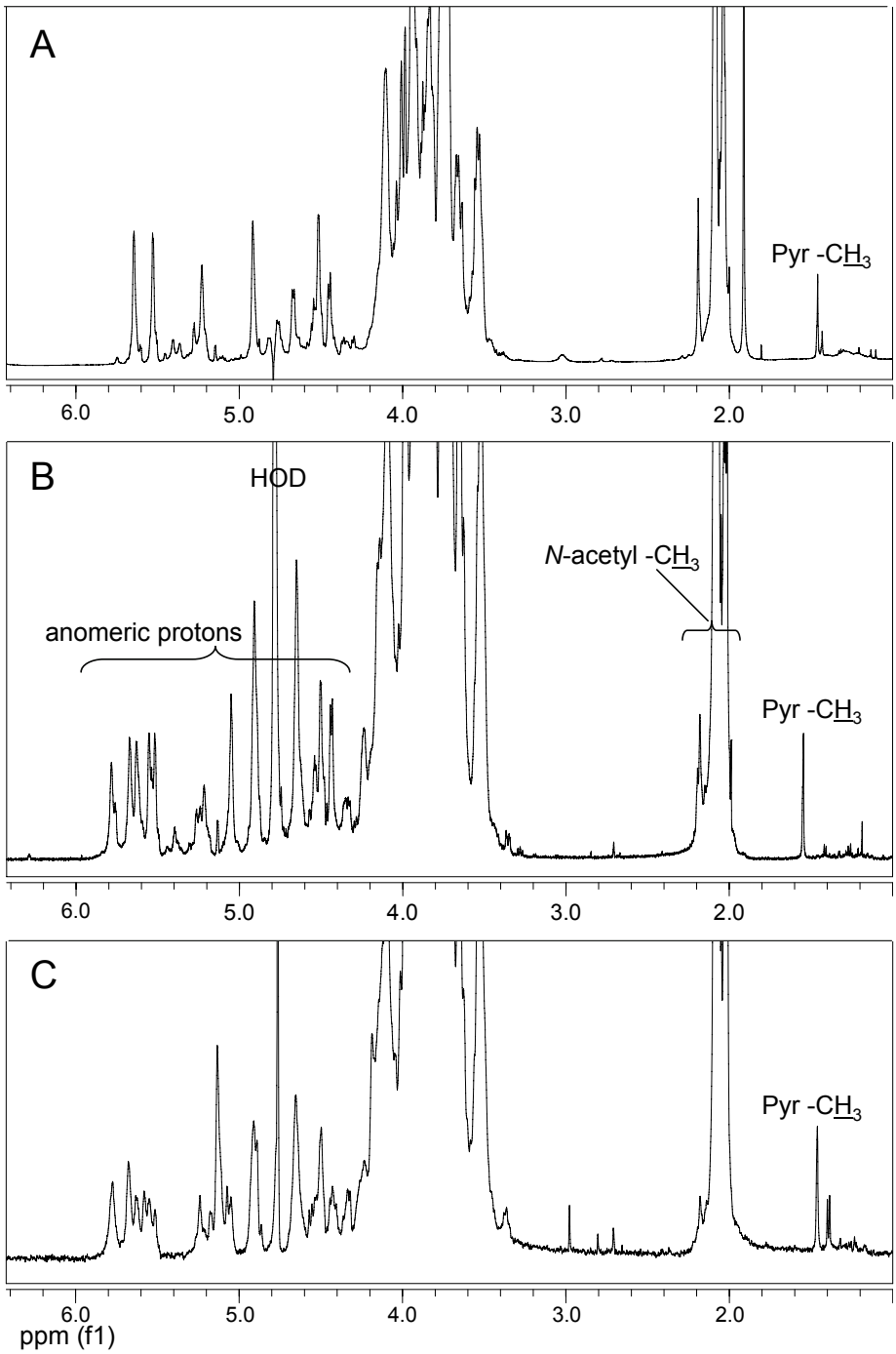

Supplemental Fig. S2

Comparison of 600-MHz proton NMR spectra for the SCWP from *B. anthracis* and pathogenic *B. cereus* strains. ***A***, *B. anthracis* Sterne 7702; ***B***, *B. cereus* G9241; and ***C***, *B. cereus* 03BB102. Significant features of the *Bc*G9241 spectrum included numerous anomeric protons (δ 5.78 – 4.30), and three major signals arising from *N*-acetyl protons (δ 2.02 – 2.09). All strains displayed a minor signal at δ 1.54 -1.47 identified as the -CH_3 protons of pyruvic acid. The *Bc*G9241 SCWP contains additional anomeric signals compared to *B. anthracis*, and the *Bc*03BB102 spectrum shows even greater heterogeneity in this region. The SCWP from *Bc*03BB87 gives the same spectrum as shown for *Bc*G9241.

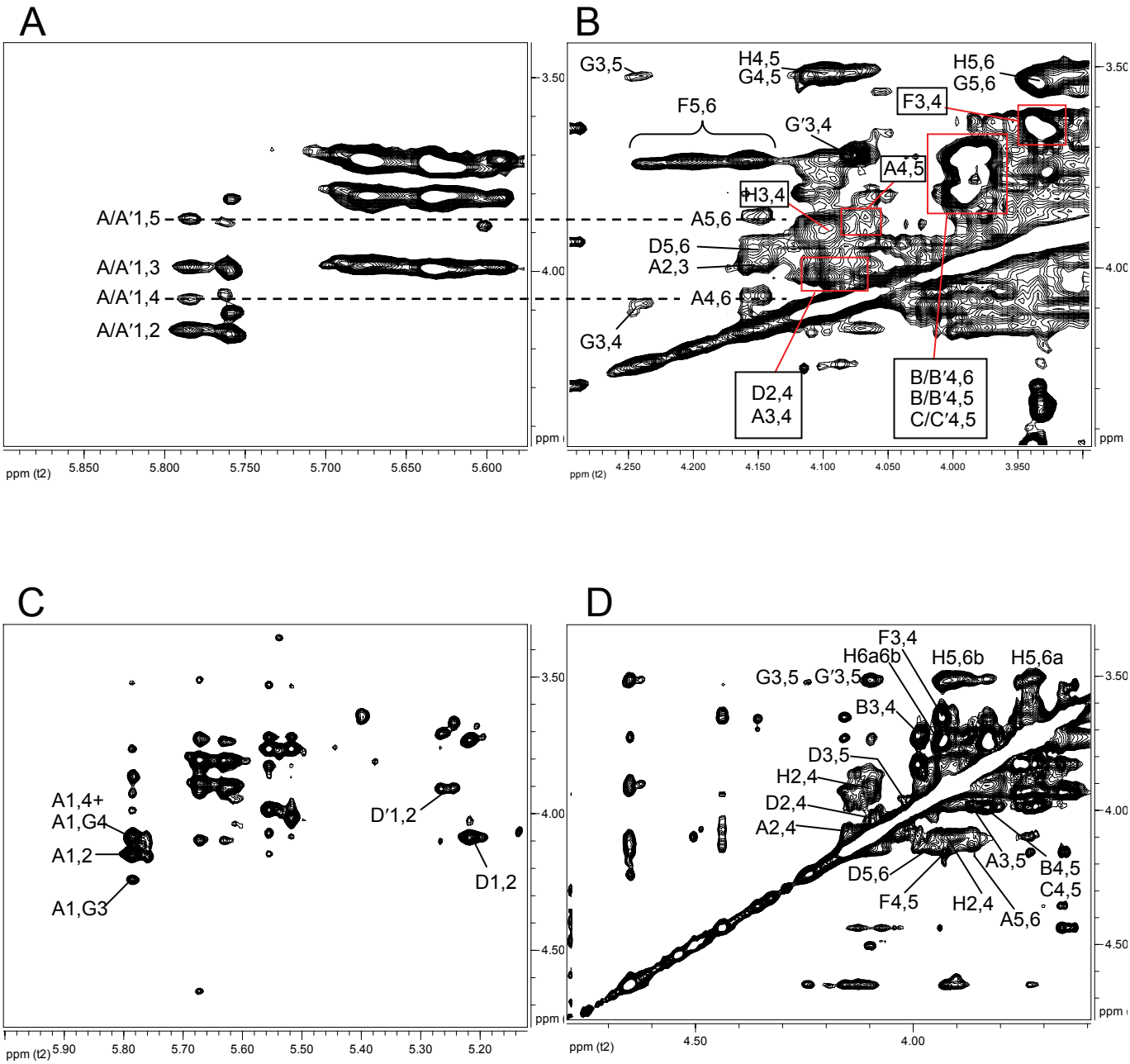

Supplemental Fig. S3
Partial 800-MHz NMR spectra of the *B. cereus* G9241 SCWP. Panels ***A*** and ***B***, ^{1}H-^{1}H-TOCSY spectra showing major ring proton scalar connectivities for residues A, B, C, D, F, G and H. Panels ***C*** and ***D***, ^{1}H-^{1}H-NOESY spectra showing major ring proton NOEs for residues A, B, C, D, F, G, and H. Additional TOCSY and NOESY connectivities involving the anomeric protons are identified in **Figs. 5**. and **6** of main text.

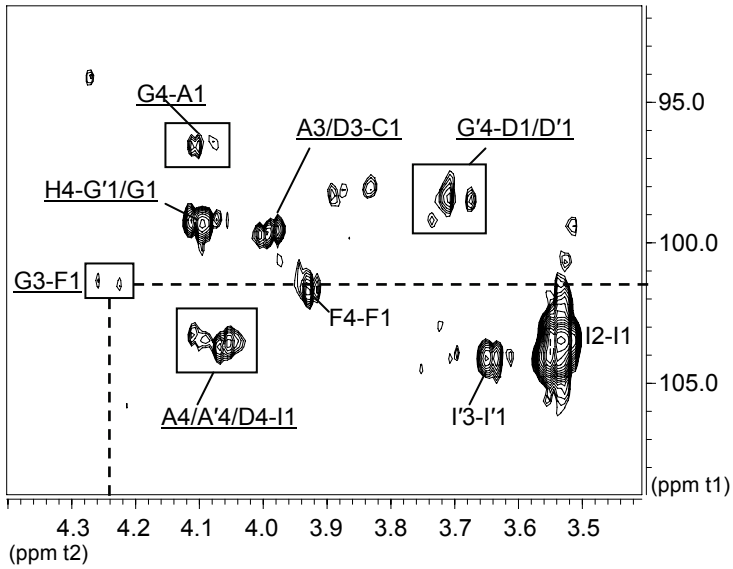

Supplemental Fig. S4
Partial 800-MHz ^{1}H-^{13}C HMBC spectrum of the *B. cereus* G9241 SCWP. The region is plotted with increased signal amplitude to allow display of the weak inter-residue correlation **G**3-**F**1. Inter-residue correlations defining glycosidic linkages are underlined. All connectivities are listed in the sequence: "proton-carbon", for example: **G**4-**A**1 designates a three-bond inter-residue correlation between H4 of residue **G** and the anomeric carbon of residue **A**. Additional connectivities are shown in **Fig. 8** of main text. Coupling intensities are not indicative of residue stoichiometry.

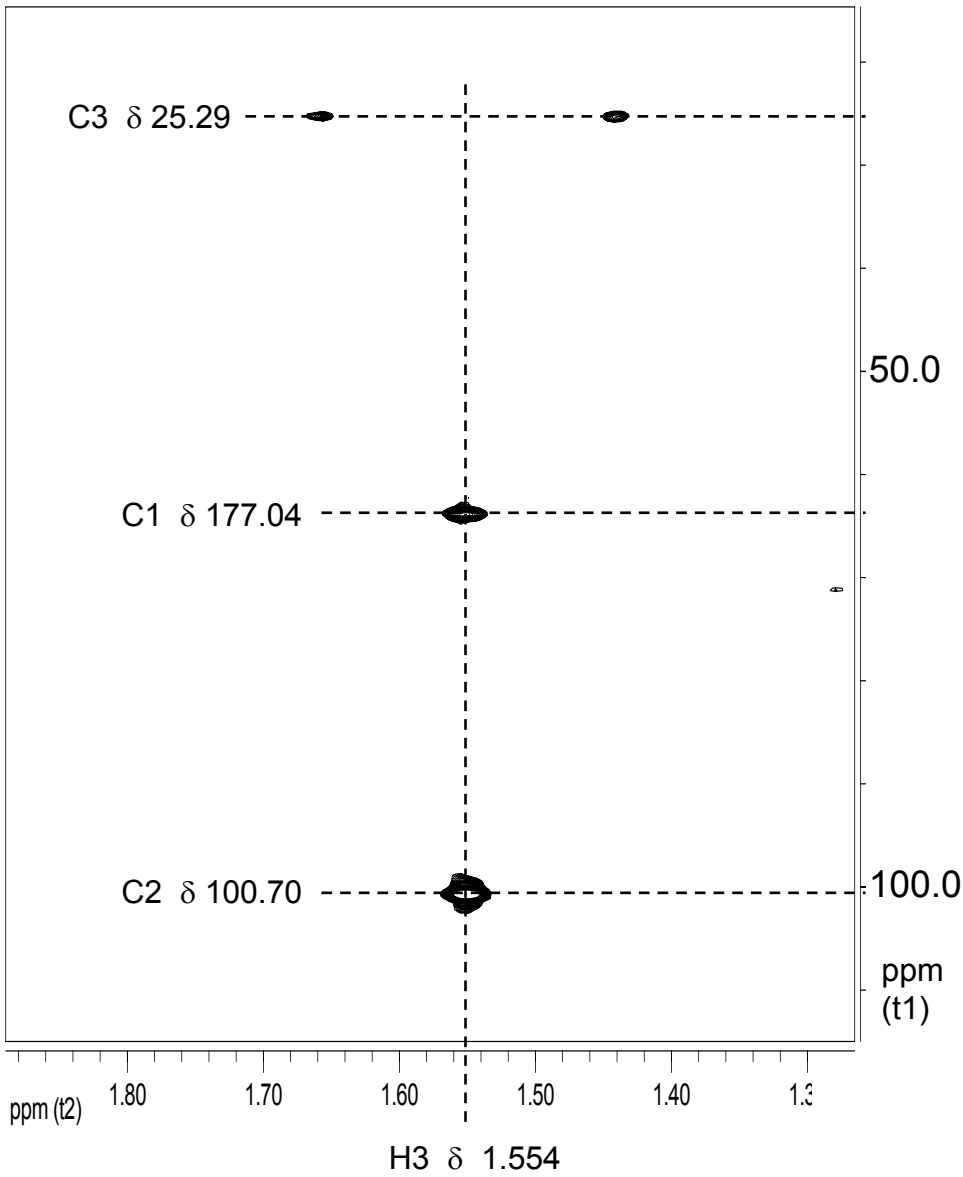

Supplemental Fig. S5
Partial ^{1}H-^{13}C HMBC spectrum of the *B. cereus* G9241 SCWP showing connectivities defining pyruvate, between the methyl group protons and carbons-1, 2, and 3. The correlation to C1 has been folded back into the displayed spectrum (calculated δ_C 177.04). Residual carbon-proton coupling at C3 results in splitting of the H3 signal.

Section --Supplementary NMR Data

α-Gal*p* residues: Summary of data for identification of α-Gal*p* residues **B/B′** and **C/C′**

The *galacto*- configuration for residues **B/B′** was assigned from COSY, TOCSY, NOESY and HSQC analyses (**Table III**). Magnetization transfer was evident from proton H1 only thru H4 in COSY and TOCSY, consistent with the *galacto*- configuration, and the remaining positions were deduced from scalar couplings between H6/H5/H4 in TOCSY and by NOEs between protons H3/H5, H3/H4, and H4/H5. The carbon shifts and observed NOEs are consistent with the α-pyranosidic ring form and $^{4}C_{1}$ conformation. Further confirmation was obtained from ^{1}H-^{13}C-HSQC-TOCSY analysis, which revealed connectivities between H4/C4 and H3/C3, and between H4/C4-H5/C5-H6/C6 for both the **B** and **C** ring systems (not shown). The $J_{C1,H1}$ coupling constants (**Table III**) were consistent with the α-anomeric configuration and the δ_C values for carbons C2 thru C6 were within range to indicate that both pairs of residues, **B/B′**, and **C/C′**, are terminal unsubstituted α-Gal pyranose residues.

β-Gal*p* residues:

Supplemental Table I Additional, minor β-Gal systems (residue **I** series) partially assigned, also refer to **Figure 4*D***; δ_H (black); δ_C (red)

I′ β-Gal	4.57 100.77	3.47	3.63 72.32	3.91 69.83[c]	3.64 74.6	Not assigned
I″ β-Gal	4.54 102.28	3.54 72.41	3.67 73.48	3.93[a] 68.33[c]	3.50[b] 74.99	3.74/3.81 60.6
I‴ β-Gal	4.35 102.92	3.55 74.93?	3.65 75.20	3.93[a] 68.98[c]	3.54[b] 74.8	Not assigned
I⁗ β-Gal	4.33 103.14	3.54 70.69	3.65 75.20	3.93[a] 70.06[c]	3.53[b] Not assigned	Not assigned

[a,b,c] assignments may be interchanged